Available online http://amq.aiqua.it
ISSN (print): 2279-7327, ISSN (online): 2279-7335

Alpine and Mediterranean Quaternary, 37 (1), 2024, 67-82 https://doi.org/10.26382/AMQ.2024.04

EVIDENCE OF ANOXIC LAYERS IN THE CENTRAL TYRRHENIAN SEA BETWEEN 29 AND 4.2 KA

Valerio Ruscito [1], Luisa Conforto [2], Luigia Manfra [2], Maria Preite Martinez [2]

1 Applied Geophysics Unit GEO-GFI, Geological Survey of Italy, ISPRA, Rome, Italy.
2 Department of Earth Sciences, Sapienza University of Rome, Rome, Italy.

Corresponding author: Valerio Ruscito <valerio.ruscito@isprambiente.it>

ABSTRACT: Heavy metals contents are analyzed in a continuous sediment record spanning from 29 to 4.2 ka BP, sampled on the upper continental slope facing the Ombrone River mouth (Tyrrhenian Sea) and investigated in previous works by isotopic and micropaleontological studies supported by radiocarbon dates. The aim of this work is to use changes in some heavy metals contents, which were shown to reflect change in the pH and Eh on the sea floor environment, to investigate the mechanism involved in the expression of bottom anoxia between 29 and 4.2 in the Central Tyrrhenian Sea. Fe, Mn, and Pb content shows significant correlations with paleoenvironmental changes. Pb elemental concentration proved to be the most powerful tool to reconstruct environmental redox conditions, being greatly enhanced during strong anoxia phases and showing conservative behavior not influenced by post depositional diagenesis. Geochemical evidence from Ombrone submerged delta sediment suggest the occurrence of two reducing phases. During the Holocene, data highlight the presence of a reducing layer in the West Mediterranean between 7.4 and 5.7 ka BP, with a climax between 6.8 and 5.7 ka BP, in agreement with previous evidence. In this period, probably, enhanced river runoff increased the flux of continental organic matter into the basin and reduced sea surface salinity, leading to the formation of an anoxic environment. The presence of this reducing layer agrees with evidence of a “pluvial” period recognized by other authors in the West-Central Mediterranean, partially synchronous with the Sapropel S1 formation in the East, suggesting its regional character and its extension to the whole Mediterranean Basin. Additionally, trace metal data suggest the occurrence of an additional anoxic phase, not previously recognized, and occurring during the Last Glacial Period, at about 27.2 ka BP.

Keywords: Reducing Layers; heavy metals; West Mediterranean Sea; Last Glacial-Middle Holocene period; paleoclimatology; inorganic geochemistry.

1. INTRODUCTION

The Mediterranean region is particularly influenced by climatic variations due to its semi-enclosed basin, being influenced by the North African subtropical climate and the temperate European westerly atmospheric circulation (e.g. Lionello et al., 2006). One of the most important type of paleoclimatic events found in this area is the deposition of reducing layers, mainly identified as Sapropels in the East Mediterranean and as Organic Rich Layers (ORLs) in the West (Rossignol-Strick, 1985; Rohling, 1994; Rogerson et al., 2008; Negri et al., 2012; Fink et al., 2013; Rohling et al., 2015; Incarbona & Sprovieri, 2020; Pérez Asensio et al., 2020). Sapropels are organic-rich layers recovered in marine sediments from many localities throughout the Eastern and central Mediterranean Basin. Kidd et al. (1978) described them as sharply defined, dark colored sedimentary layers with a C org content > 2 wt.% and thickness >1 cm. ORL are defined as dark sediment layers with total organic carbon (TOC) content up to 1 wt.% (Rogerson et al., 2008; Negri et al., 2012; Fink et al., 2013).

Sapropelic layers occur almost periodically in the sediments of the last 13.5 million years in the Mediterranean Sea, more often developed in the Eastern than in the Western sub-basins (Rohling et al., 2015). The Holocene Sapropel S1 has been widely identified in the Eastern Mediterranean. Its formation is primarily due to the increased fluvial discharge from the Nile River and the Central Saharan Watershed (Rossignol-Strick et al., 1982; Gallego-Torres et al., 2010; Williams et al. 2015; Blanchet et al., 2021), linked to enhanced monsoonal activity over equatorial Africa, with a partial contribution of increased precipitation in the Mediterranean region including its northern borderlands (Rohling & Hilgen, 1991; Kotthoff et al., 2008; Geraga et al., 2010; Toucanne et al., 2015; Wu et al., 2017). In the East Mediterranean, S1 broadly spans from 10.8 cal ka BP to 5.5 cal ka BP, separated in two distinct phases (S1a and S1b) with a short interruption roughly centered at 8 cal ka BP (Kotthoff et al., 2008; Geraga et al., 2010; Hennekam et al., 2014; Triantaphyllou et al., 2014; Grimm et al., 2015; Filippidi et al., 2016; Wu et al., 2017; Di Donato et al., 2019; Wu et al., 2019).

West Mediterranean ORLs could be considered as weakly expressed sapropels (Rogerson et al., 2008), corresponding to anoxic phases, linked to water stagnation and enhanced biological production that depletes the available oxygen (Grimm et al., 2015). These anoxic phases may have been originated by hydrological and productivity changes related to the Atlantic inflow from the Gibraltar strait that could have induced the reduction

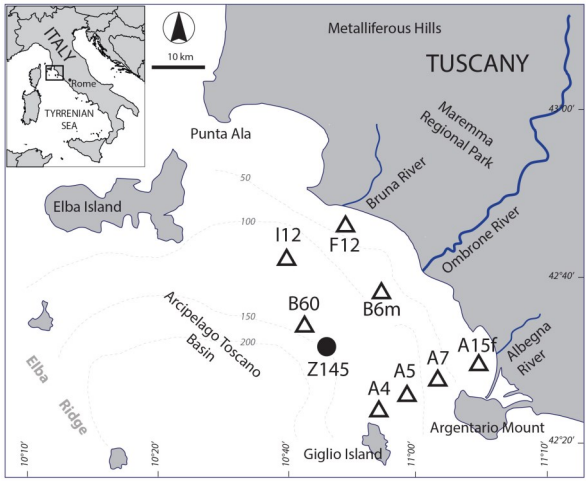

Fig. 1 - Map of the study area and samples locations. Black dot indicates the core Z145 (150 m depth, Lat. 42°32'15" N, Long. 10°47'47" E), sampled on the upper continental slope about 22 km SW off the present-day Ombrone River mouth. Open triangles show the eight box-cores sampled on recent sediments of the continental shelf.

of the deep circulation (Rohling et al., 2015). They also could derive from an enhanced river runoff, following the deglaciation and the alpine ice melting, or from an increasing precipitation regime that caused a decrease in surface salinity (Rogerson et al., 2008; Rohling et al., 2015; Grant et al., 2016; Bakrač et al., 2018; Bazzicalupo et al., 2018; Pasquier et al., 2019). The great influence of the North Atlantic climate on western Mediterranean hydrological activity is demonstrated by many other authors (Bard et al., 2002; Zanchetta et al., 2007; Toucanne et al., 2015; Pasquier et al., 2019; Wagner et al, 2019).

Late Glacial-Holocene anoxia periods, leading to ORL deposition, are found in the Alboran Sea, spanning from 15 to 8.5 ka BP (Rogerson et al., 2008; Fink et al., 2013; Jimenez-Espejo et al., 2015; Dubois-Dauphin et al., 2017; Bazzicalupo et al., 2018), in the Gulf of Lion (Pasquier et al., 2019) and in the Ligurian Sea spanning from 15 to 11 ka BP and from 11 to 6 ka BP (Le Houedec et al., 2021). All these studies prove an important enhance of freshwater runoff from northern borderland in the west Mediterranean Basin. At present the runoff in this region mainly depends on the North Atlantic atmospheric circulation and is affected by local orography of the coasts (Trigo et al., 2002; Kandiano et al., 2014).

The present work focuses on climatic changes recorded in several cores collected in the Arcipelago Toscano Basin, in the Central Tyrrhenian Sea, near the Ombrone River mouth (Fig. 1). One of the core was previously investigated by oxygen isotope analyses on foraminifera and micropaleonotological analyses, together with radiocarbon age determinations (Belluomini et al., 2002; Carboni et al., 2005).

The aim of this work is to use changes in some heavy metal contentsome heavy metalselago Toscano b, which were shown to reflect change in the pH and Eh on the sea floor environment, to investigate the mechanism involved in the expression of bottom anoxia between 29 and 4.2 in the Central Tyrrhenian Sea (Fig. 1). (Thomson et al., 1995; Warning & Brumsack, 2000; Naimo et al., 2005; Reitz et al., 2006; Tribovillard et al., 2006; Angelidis et al., 2011; Heimbürger et al., 2012; Oliveri et al., 2013; Jiménez-Espejo et al., 2015; Martinez-Ruiz et al., 2015). This approach is suggested by previous works (Conforto & Manfra, 2004; Conforto & Manfra, 2007; Conforto et al., 2008), that evidenced significant correlations between heavy metals behaviors and paleoclimatic changes. New geochemical analyses, reported in this work, together with a review of previous geochronological, isotopic, sedimentologic and micropaleontological results, allowed a more detailed paleoenvironmental reconstruction of this area.

2. STUDY AREA AND MATERIAL

The studied area (Fig. 1) is comprised between the 200 m isobath and the Tuscany coast, in the Arcipelago Toscano National Park area. It is limited on the south by the Argentario Mount and Giglio Island, extending northward to Punta Ala and Elba Island in the Tuscan mining district (Elba Island and Metalliferous Hills on the mainland). The continental shelf receives terrestrial sediment supply mainly discharged from the Ombrone River (monthly min/max mean discharge 4/50 m^3/s) (Bellotti et al., 2004). The role of the minor rivers (Bruna and Albenga) is subordinate. The Ombrone River is 161 km long and drains a basin of 3496 km^2 characterized by phyllites, quartzites, arenites, siliceous and carbonate sequence, Plio-Pleistocene clayey-sandy sediments, ophiolitic sequences and trachyandesite volcanics (Bellotti et al., 2004).

At present, the Ombrone mouth is a wave-dominated delta consisting of fine sand to clay sediments (Tortora et al., 1999; Bergamin et al. 2001). Coarser fluvial sediments are distributed mainly northward by longshore currents, while finer ones drape the shelf (Aiello et al., 1975; Tortora, 1999).

This area was shown to be ideal for Quaternary paleoclimatology studies based on geological and geochemical analyses (Belluomini et al., 2002; Carboni et al., 2005), due to its geomorphological condition of a semi-enclosed basin. A submerged structural high, called Elba Ridge, delimits the shelf to the western side and has a great impact on the morphologic and sedimentary setting of the area, both presently and during the late Quaternary sea-level lowstand (Roveri & Correggiari, 2004).

Geochemical analyses were performed on the Z145 core, located on the upper continental slope at about 22 km SW off the Ombrone River mouth, at a depth of 150.8 m (Fig. 1). During the Last Glacial Maximum (LGM), the continental shelf was largely exposed, and the distance between the Z145 sampling site and the Ombrone mouth was only about 7 km (Alessio et al., 1994). During the last deglaciation, the sea level rise and the following stabilization (3.5-3.0 ka BP) caused the eastward migration of the Ombrone river mouth, and a lagoonal delta system developed (Carboni et al., 2005).

Z145 core is about 4 m long and spans continuous-

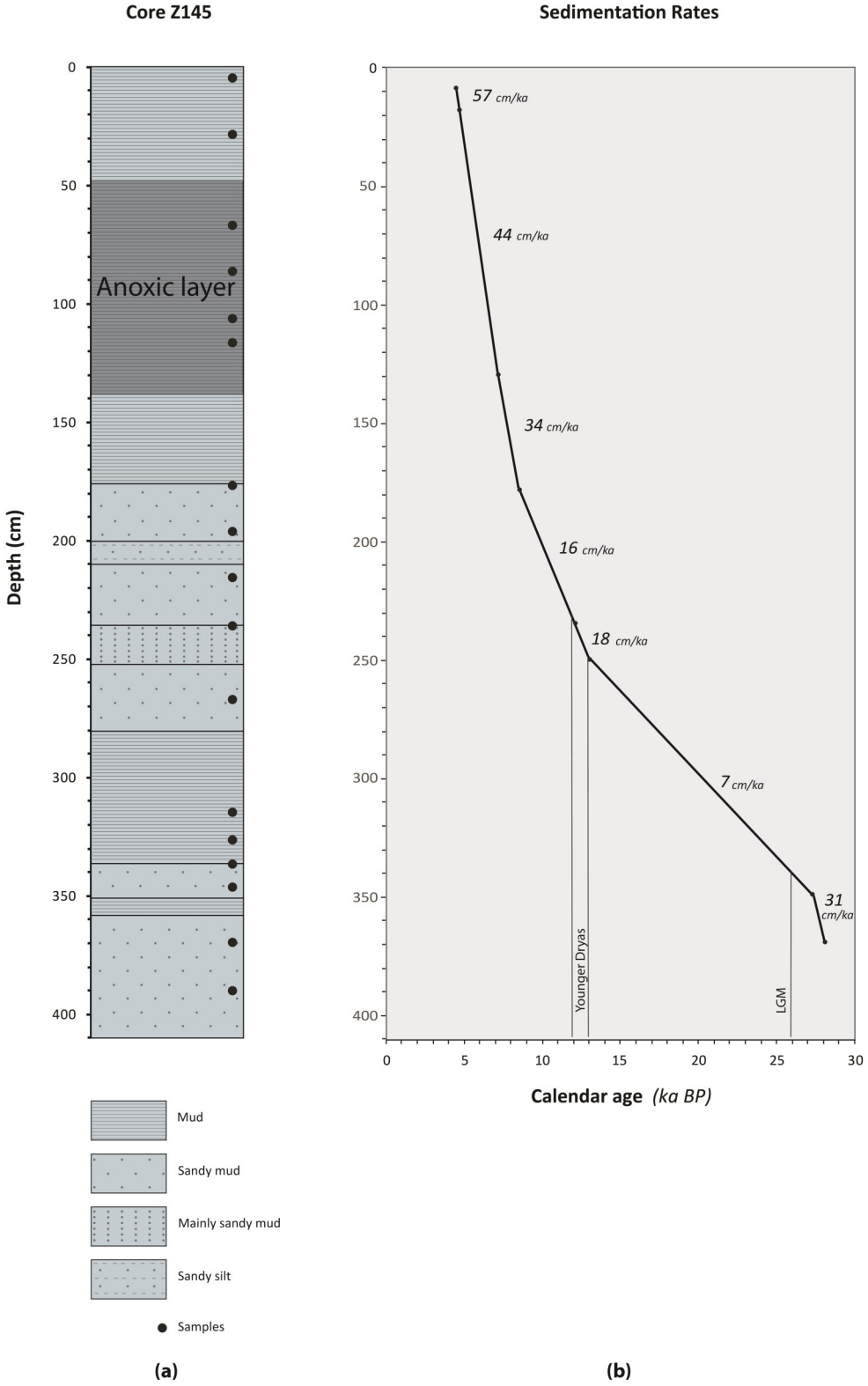

Fig. 2 - a) Lithological log of core Z145 and samples analyzed in this study (●). b) Sedimentation Rate (SR) is calculated using measured radiocarbon dates. Modified from Carboni et al. (2005).

ly from about 29 to 4.2 cal ka BP. To know the present heavy metals background in the area, analyses were also carried on recent sediments sampled in 8 box-cores (A4, A5, A7, B60, B6m, F12, I12 and A15f), collected on the continental shelf (Fig. 1). Core B60 is the site nearest to Z145 and represents a good candidate to study the recent sediments at the top of the Z145, that were lost during sampling.

The Z145 sediment consists mainly of grey mud in the upper part of the core, and of an alternation of muddy and sandy mud levels below 180 cm. The detailed log and sedimentological features of Z145 core are reported in Carboni et al. (2005), together with isotopic ($\delta^{18}O$ on foraminifera) and micropaleontological results. The record is anchored to an age model supported by seven radiocarbon dates (Carboni et al., 2005).

The sedimentation rate (SR) in Z145 is very low during the Glacial period, sharply increases in the Younger Dryas and reaches the highest value at about 7.5 cal ka BP, when anoxia conditions established (Fig. 2). The eight small cores of recent sediments are about 15 cm long (A4, A5, A7, B60, B6m, F12, I12, A15f) and are mainly composed of silty clay. They are dated between 1950 and 1992 by ^{137}Cs and ^{210}Pb methods (Belluomini et al., 2002).

3. PREVIOUS PALEOCLIMATIC EVIDENCES

The previous analyses carried on Z145 core allow the paleoclimatic reconstruction for this area. Basing on micropaleontological and isotopic evidence, Carboni et al. (2005) identify the Glacial period in the bottom layers, and the LGM at about 26 cal ka BP (Tab. 1 and Fig. 3, dates recalibrated in this work), according to Ivy-Ochs et al. (2008), McCullock et al. (2010), Shakun et al. (2010), Adamson et al. (2013), Domnguez-Villar et al. (2013), Sarikaya et al. (2015), Oliva et al. (2018) and Seguinot et al. (2018).

Z145 proxies identify also the Younger Dryas cold event, spanning from about 12.9 cal ka BP to 11.7 cal ka BP, according to several authors (Ivy-Ochs et al., 2008; McCullock et al., 2010; Fiedel, 2011; Carlson, 2013; Fink et al., 2013; Kennet et al., 2015; Beyin et al., 2017; Bazzicalupo et al., 2018; Gromig et al., 2018; Keigwin et al., 2018; Oliva et al., 2018; Pauly et al., 2018; Ribolini e al., 2018).

A cooler period is highlighted between 8.8 and 7.4 cal ka BP, synchronous with the cooling event recorded at 8.2 cal ka BP, according to several authors (Rohling & Pälike, 2005; Spötl et al., 2010; Magny et al., 2011; Rodrigo-Gàmiz et al., 2011; Lirer et al., 2013; Schemmel et al., 2016).

A warm and wet period with stratified oligotrophic waters occurred from 7.4 cal ka BP until about 5.2 cal ka BP. Micropaleontological data suggest anoxic condition, likely related to a hard rainy phase, spanning about 1000 years, established on the borderland of western Mediterranean basin, as recognized in Croatia (Bakrač et al., 2018) and in SW Spain (Schröder et al., 2018). After the anoxic event, bottom water oxygenation re-established, and climatic conditions changed in a drier and cooler period corresponding to the top of the core and placed at about 4.2 cal ka BP, in agreement with

Depth (cm)	Age14C (a BP)	Calendar age marine reservoir (a BP)	δ18O (‰ vs PDB)
0.5*		4260	
1*		4270	
1.5*		4280	
2.5*		4290	
3		4300	0,74
3.5*		4310	
4.5*		4330	
5*		4340	
6*		4360	
8*		4390	
10	4282±33a	4233- 4617; M.P. = 4430	
18	4388±94 b	4279 -4836; M.P. = 4570	
29*		4820	
38		5020	0,79
48		5250	
58		5580	
68*		5710	-0,03
78		5940	0,16
88*		6170	0,16
98		6390	0,31
108*		6620	0,33
118*		6850	0,06
128		7080	0,15
130	6643±52 a	6929- 7303; M.P. = 7120	
138		7360	0,55
148		7650	
158		7940	0,32
178*	8034±121 b	8215- 8899; M.P. = 8530	
183		8850	0,17
198*		9810	-0,19
208		10450	-0,18
215*		10900	
218		11090	-0,31
228		11730	0,06
235	10723±74 a	11880-12469; M.P. = 12180	
238		12350	0,58
248*		12910	2,78
250	11537±74 a	12806 -13227; M.P. = 13020	
258		14180	2,56
268*		15630	1,88
278		17080	2,82
288		18530	
298		19980	
308		21430	
315*		22440	
318		22880	2,18
328*		24330	
338*		25770	3,04
348*		27220	1,96
350	24060±300 a	27005 -28221; M.P. = 27550	
358		27810	2,85
370*	24710±220 a	27714 - 28695; M.P. = 28200	
390*		28840	
409		29460	2,76

Tab. 1 - Z145 radiocarbon dates (from Carboni et al., 2005, modified using Reimer et al., 2020 calibration curves). a = AMS dates; b = LSC dates; M.P. = Median Probability. Dated control points are shown in bold and dates in italics are extrapolated and approximated to 10 years. In the first column, asterisks (*) indicate the chemically analyzed levels. Geochemical data: $\delta^{18}O$ of *G. bulloides* (from Carboni et al., 2005).

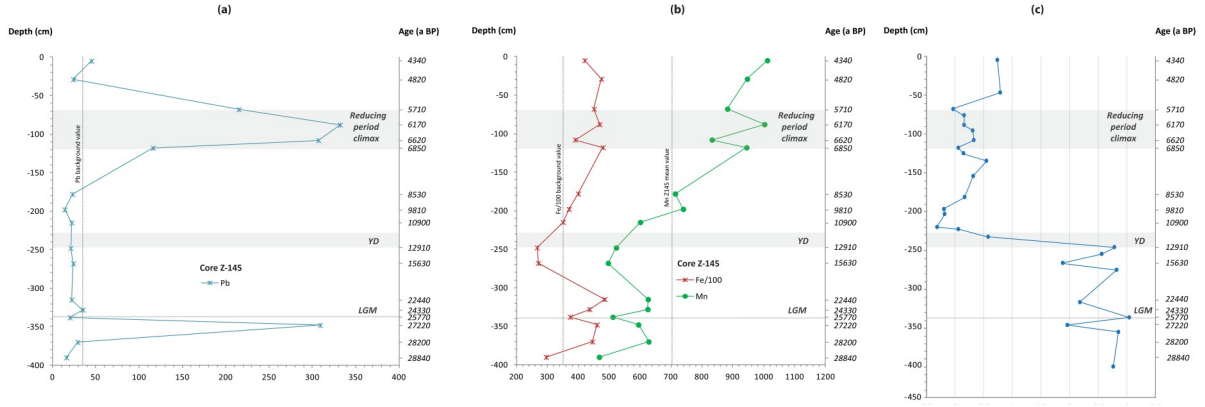

Fig. 3 - Heavy metals concentration in core Z145. a) Pb concentration curve. b) Fe/100 and Mn concentration curves, their data are reported using different scales. c) *G. Bulloides* $\delta^{18}O$ values from Carboni et al (2005). Points mark the analyzed samples (see Tab. 1). The grey areas show the Younger Dryas and reducing climax periods, the grey line indicates the Last Glacial Maximum (LGM). Pb and Fe recent background are reported. Mn mean value is calculated from Glacial and Holocene Z145 means.

several authors (Melki et al., 2009; Colonese et al., 2013; Lirer et al., 2013; Di Rita et al., 2018; Schröder et al., 2018; Bini et al., 2019; Isola et al., 2019).

During the mid-Holocene period, Magny et al. (2011), Colonese et al. (2013) and Di Rita et al. (2018) identify a paleoclimatic limit, between the SE/NW Mediterranean regions, placed at 40-42° N, characterized by wetter winters in the northern areas and humid summers in the southern. As the Z145 core is situated at 42° 35'N, the study area is likely mainly representative of the climatic situation of the Northern Mediterranean region, perhaps with some influences from the Southern.

4. MATERIALS AND METHODS

Analyses of Fe, Mn and Pb concentrations were performed on 17 sediment samples from core Z145 and on 8 samples from the box-cores, using an ICP-AES housed in the Earth Science Department of the Sapienza University (Rome). Instrumental errors mainly range between 1-15%. Total concentrations were determined following a strong hot acidic attack using mixtures of perchloric and hydrofluoric acids. A sequential extraction to measure metals partitioning into the main fractions was performed following the method proposed by Sahuquillo et al. (1999). In order to improve the knowledge of the elements behaviors in different environmental conditions, we directly measured concentrations in the carbonate, oxides and organic partial fractions, while the residual content has been determined as difference. Not all oxides, mostly the Fe oxides, could be dissolved in this sequential analysis (Fletcher, 1981), the metals easily removable (i.e. adsorbed on the clay minerals) are comprised in the carbonate fraction.

Radiocarbon dates of core Z145 (from Carboni et al., 2005) are recalibrated using the marine calibration curve IntCal20 (Reimer et al., 2020) and expressed as calendar marine ages with a reservoir age correction of 400 yrs. Isotopic values are reported following new ages calibration. (Tab. 1). For the micropaleontologic data see Carboni (2005).

5. RESULTS AND DATA INTERPRETATION

Table 1 report $\delta^{18}O$ data and radiocarbon ages determination for core Z145, presented in Carboni et al. (2005). Tables 2-6 show concentrations values of Fe, Mn and Pb of the analyzed samples from Z145 core, used for the paleoclimatic reconstruction, and from the 8 box-cores (Fig. 1), which provide information about the recent background of these elements in the area. Great significance has the box-core B60 because it is the site nearest to Z145 and represents a good candidate to study the top sediments lost during Z145 sampling.

Our data allow a detailed study of geochemical behavior of Pb, Mn and Fe in order to obtain a better reconstruction of paleoenvironmental conditions in the Ombrone delta submerged area. Concerning the general behavior of elements in various pH and Eh conditions see Glasby (2006), Mihaljevic (1999), Williamson (1999).

Overall, variations in Pb, Mn and Fe content studied in the Z145 record are in good agreement with the previously identified climatic phases (see Sec.3) from the last Glacial Period until 4.2 cal ka BP, allowing often a better delimitation of their boundaries (Fig. 3).

5.1. Pb

In core Z145, Pb shows highly enhanced values both in the Glacial and the Holocene periods. During the Holocene, the distribution of Pb (Tab. 2a and Fig. 3a) shows a concentration increase between 6.8 and 5.7 cal ka BP, with a peak zone mean of 246 ppm, reaching its maximum at 6.2 cal ka BP (332 ppm). These values are clearly anomalous: the peak value is about 13 times higher than the mean (26 ppm) of the other values during the Holocene. Moreover, these values are about six times the B60 mean (56 ppm, Tab. 3), and about nine times the present background in the area (35 ppm, Tab. 4). In these levels, the sedimentation rate (SR) (Fig. 2) increases to 44 cm/ka, while at the beginning of the Holocene it was about 22 cm/ka (see Fig. 3a). Overall, there is not a strict correlation between Pb variation and

(a)	Depth (cm)	5	29	68	88	108	118	178	198	215	Average
	Age (a BP)	4340	4820	5710	6170	6620	6850	8510	9810	10900	(ppm)
	Pb (ppm)	45	24	215	332	307	116	23	14	22	122
	Fe/100 (ppm)	420	474	450	469	389	479	399	369	350	422
	Mn (ppm)	1011	946	882	1002	832	944	713	739	600	852

(b)	Depth (cm)	248	268	315	328	338	348	370	390	Average
	Age (a BP)	12910	15630	22440	24330	25770	27220	28200	28840	(ppm)
	Pb (ppm)	21	24	22	35	20	309	29	16	24
	Fe/100 (ppm)	266	270	485	436	373	460	445	295	379
	Mn (ppm)	522	496	625	624	511	594	627	467	558

Tab. 2 - Heavy metals concentrations in core Z145. a) Holocene samples. Top record does not coincide with the seafloor as the top sediments were lost during sampling. b) Glacial samples. Ages are calculated from control points (Tab. 1).

Age (yr AD)	1991	1988	1985	1980	1970	1952	Average
Depth (cm)	0,5	1	1,5	2,5	4,5	8	(ppm)
Pb (ppm)	61	57	58	54	52	52	56
Fe/100 (ppm)	373	384	351	379	376	377	372
Mn (ppm)	3795	3830	3026	1436	1026	1173	2381

Tab. 3 - Pb, Fe/100, Mn concentrations in B60 box-core.

Site	A4	A5	A7	B60	B6m	F12	I12	A15f	
									Background (ppm)
Pb (ppm)	49	4	50	56	40	17	43	24	35
Fe/100 (ppm)	354	354	381	373	387	267	362	357	355
Mn (ppm)	1080	879	711	2381	1099	706	1588	548	1124

Tab. 4 - Pb, Fe, Mn mean values in recent samples (box-cores). The last column shows the present background of the area, calculated from all of the sites means.

SR trend throughout the entire record, indicating that probably Pb anomalies are not primarily driven by increases in inland sedimentary contribution. The high Pb values probably are due to environmental conditions with low redox potential (Eh), where the bacterial activity reduces the sulfates to sulfides, leading to the precipitation of Pb as PbS (Zhang et al., 2014; Turner et al., 1986). PbS is not influenced by post depositional reoxidation, as its solubility product is the lowest, after HgS, among metallic elements sulfides. The reducing conditions are probably due to an enhanced freshwater input that, together with following reduced sea surface salinity highlighted by the isotope data, hampered the bottom water levels oxygenation. This is in good agreement with Drab (2015), who found heavy metals sulfides increase in two sapropels in the Marmara Sea.

	Z145		B60		
Depth (cm)	108	215	0,5	1,5	8
Pb carb. (%)	1	0	2	5	6
Pb ox. (%)	1	9	5	7	5
Pb org. (%)	10	34	63	49	53
Pb residual (%)	88	57	30	39	36
Mn carb. (%)	63	26	49	74	74
Mn ox. (%)	0	41	41	12	16
Mn org.(%)	6	9	9	3	7
Mn residual (%)	31	24	1	11	3
Fe carb. (%)	0	0	0	0	0
Fe ox. (%)	4	0	3	4	3
Fe org.(%)	0	1	1	1	1
Fe residual (%)	96	99	96	95	96

Tab. 5 - Pb, Mn, Fe percentage distributions in the partial fractions in core Z145 and in box-core B60. In Z154, level at 108 cm corresponds to the reducing layer, level at 215 cm corresponds to the beginning of the Holocene.

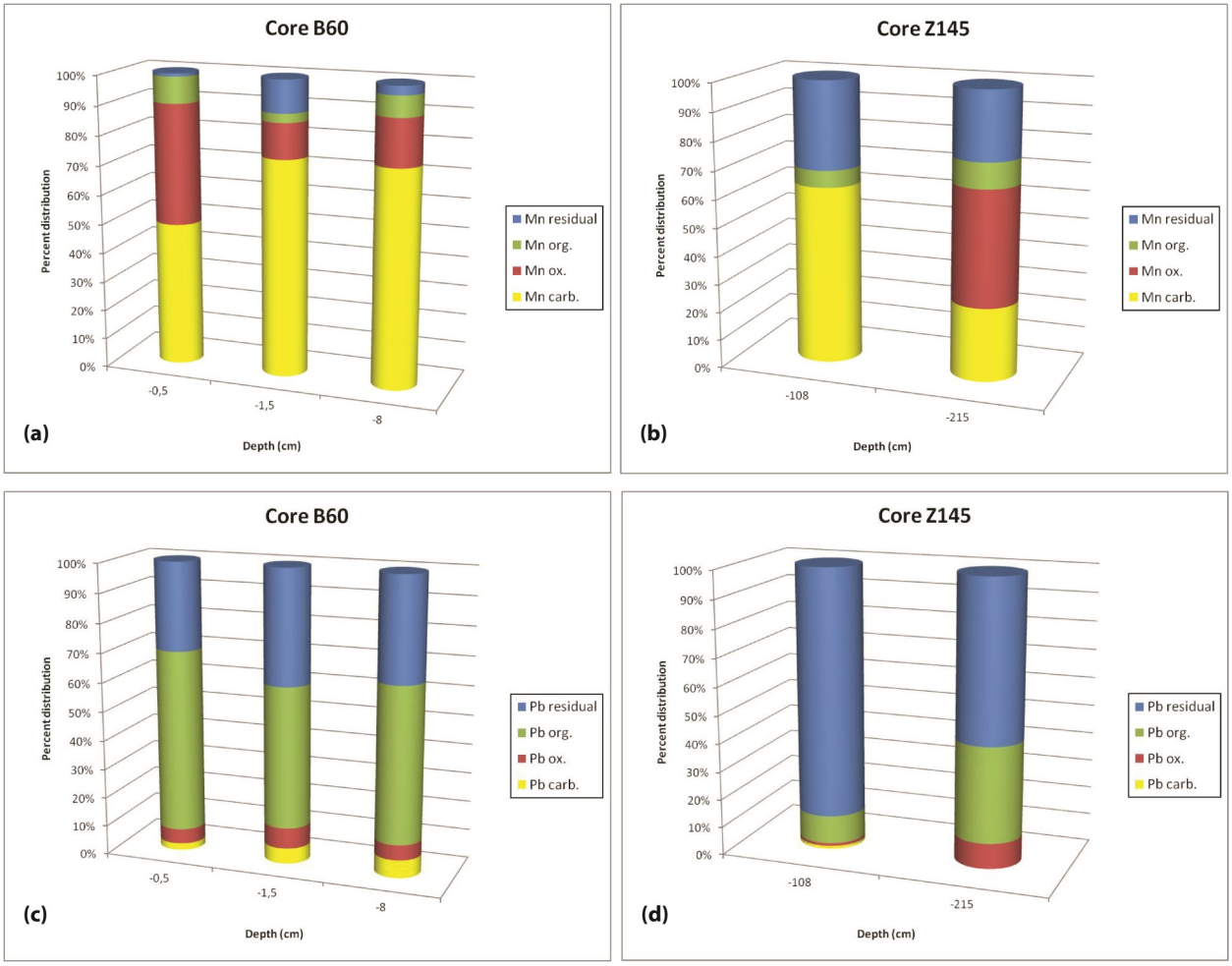

Fig. 4 - Pb and Mn percentage distribution in partial fractions: a) Mn in B60; b) Mn in Z145; c) Pb in B60; d) Pb in Z145.

Another high Pb concentration value is also measured during the Late Glacial, at about 27.2 cal ka BP (Tab. 2b and Fig. 3a). Here, Pb reaches 309 ppm, a value close to higher Holocene contents and about 13 times higher than the mean of other Glacial values (24 ppm). Environmental conditions in the study area were very different between the two periods. During the Glacial, the Ombrone River flowed into the Tyrrhenian Sea several kilometers closer to the Z145 site, increasing the supply from the coastal environment, although the hydrological cycle and the river runoff could have been weaker than during Holocene times. Although only one sample is here available, because of the low sedimentation rate, as Pb value is very similar to the Holocene ones, we can hypothesize also in this glacial interval the presence of a reducing layer.

The Pb behavior in the partial fractions from cores Z145 and B60 is also investigated (Tab. 5). In Z145, values are measured at-108 cm, corresponding to the reducing layer, and at -215 cm, corresponding to the beginning of the Holocene (Fig. 4d). Pb mainly concentrates in the residual (88% at - 108 cm and 57% at -215 cm) and organic (10 at - 108 cm and 34% at -215 cm) fractions and to a lesser extent in the oxides and in the carbonate. At the -108 cm level its values reach about 90% in the residual phase, being only 10% in the organic one, and close to zero in the two other phases. These values support the notion of an anoxic environment, causing a remarkable Pb precipitation as PbS. During chemical sequential extraction, PbS is dissolved after the oxidizing step, with following precipitation as $PbSO_4$ enriched in the residual phase (Cappuyns et al., 2007). This evidence confirms the attribution of the level at -108 cm to an anoxic period, when reducing conditions were strong enough to hamper the presence of Pb in the oxide and carbonate phases. In the older level at -215 cm, Pb shows higher values in the organic and oxide phases, suggesting a presence of a more oxidized environment.

In B60 (Tab. 5, Fig. 4c), Pb concentrates mainly in the organic and residual fractions and this distribution differs from the Z145 samples. This is probably due to the diagenesis of the organic matter in the older Z145 sediments. Pb partition in the oxide and carbonate fractions shows not very significant differences between the two cores, considering that absolute values are about only a few ppm.

All data suggest that Pb is a very sensitive proxy to

identify environmental sapropel-type conditions, highlighted by Pb concentrations reaching high anomalous values. It must be emphasized that Pb content in these layers is about 9 times the present background, even though this area in the last century has been affected by anthropic pollution, mainly from mining activities and lead-added fuel. Evidence confirms that the anomalous concentrations in Z145 were exceptionally high compared to present background values, suggesting that Holocene, and probably Glacial, reducing layers conditions were strongly different than the present.

5.2. Mn

During the Holocene, in the Z145 core Mn concentration has a mean value of 852 ppm and increases toward the top of the core (Tab. 2a, Fig. 3b). This feature is due to a remobilization of Mn in the deeper, more reducing, levels and its upward diffusion and re-oxidation (Petrie, 1999). During sedimentation indeed Mn is stripped from the sediments and moves to the surficial layers (Callender, 2003; Glasby, 2006). In reducing conditions, Mn oxyhydroxide precipitation is inhibited (the lowest Mn value, during this phase is measured at 6.6 cal ka BP) enhancing the concentration of Mn^{+2} dissolved in pore water. Above reducing levels, higher Mn precipitation occurs during more oxidizing environmental conditions. The subsequent bioturbation of the superficial sediments brought downwards O_2 rich waters that oxidized dissolved Mn, causing to the formation of a secondary Mn peak at 6.2 cal ka BP, still within the anoxic layer previously identified (Thomson, 1995; Reitz et al., 2006; Rey et al., 2008; Angelidis et al., 2011; Martinez-Ruiz et al., 2015).

During the Glacial period (Tab. 2b, Fig. 3b), despite the lower sedimentation rate which causes a scarcer resolution in the sedimentary record, there is evidence of some Mn variations mostly due to glacial climatic fluctuations (Svensson et al., 2008; Guilizzoni et al., 2014; Oliva et al., 2018) that influenced the environmental and geochemical parameters (depth, distance from coast, temperature, organic substance, river supplies, pH, Eh, etc.). Tab. 2b and Fig. 3b show two Glacial Mn maximum values (28.2; 22.4 cal ka BP), separated by a minimum at 26 cal ka BP, synchronous with the LGM. Mn behaves similarly during the Holocene reducing phase, but its re-oxidation begins slightly after the end of the anoxic period identified by high Pb values. This delay is probably due to the location of the site nearer to the coast during the Glacial period, where the lower pH values hampered the Mn precipitation until the environment became oxidizing enough (Glasby, 2006). Moreover, as “true” marine geochemical conditions (Eh, pH, etc.) were not fully attained throughout the Glacial period, there is not an increasing trend upwards, as showed by the Glacial Mn mean which is only 558 ppm, much lower than in the Holocene (852 ppm).

In recent sediments of core B60 (Tab. 3), Mn reaches very high values in the top levels due to its remobilization from deeper levels and its upward diffusion and re-oxidation. During the Holocene, Mn behaviors in B60 and in Z145 are similar, but in B60 the oxidation process is stronger because the sampled levels are found in the more oxygenated surficial layers at the water-sediment interface, whereas the top levels of core Z145 were lost during sampling.

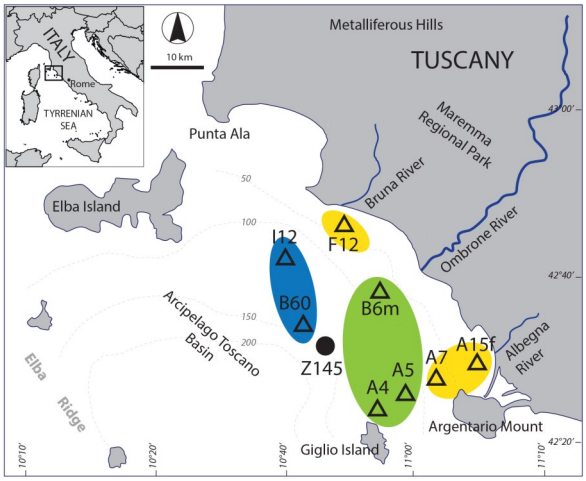

Fig. 5 - Map of Mn mean concentration areas in recent sediments of the study area. Blue area = Mn concentration between 2500 and 1500 ppm. Green area = Mn concentration between 1500 and 800 ppm. Yellow area = Mn concentration between 800 and 500 ppm.

Mn geochemical behavior is also evidenced by comparing its mean concentration in B60 to the Mn means at other sites of recent deposition (see Tab. 4). Mn means can be roughly grouped into three different areas (Fig. 5). In the first area (B60 and I12) Mn reaches its highest values. In the inner area (A15f, A7 and F12) Mn has the lowest concentrations of the whole basin. In the central area (A4, A5, and B6m), Mn has intermediate concentrations. Mn distribution therefore depends on the distance to the coast. A15f, A7 and F12 are more influenced by coastal environment and the river inputs (pH, Eh, wave energy, sedimentation, etc.) and have low Mn precipitation. B60 and I12, conversely, are in more marine environment where Mn oxide precipitation is favored. A4, A5, and B6m in the intermediate environment show intermediate concentration values. This pattern is consistent with the two different Mn features in Z145 during Glacial and Holocene times, when the distance to coast varied (Glasby, 2006).

In level -108 cm (corresponding to the Holocene reducing layer) and in level -215 cm (corresponding to the beginning of the Holocene), Mn reaches the lowest concentrations (6-9%) in the organic fraction and it shows similar values (24-31%) in the residual fraction (Tab. 5, Fig. 4b). The sum of percentage values of the oxidized and carbonate fractions is nearly constant (63-67%), the Mn distribution in each fraction being influenced by its oxidation state (Mn +2 in carbonate phase and Mn +4 in oxi-hydroxides minerals). At -108 cm (6.7 cal ka BP), Mn is mainly concentrated in the carbonate phase, in agreement with the recognized environmental anoxic conditions that hampered the formation of Mn oxides (Petrie, 1999; Callender, 2003; Glasby, 2006). It must be emphasized that during the anoxic period the environmental reducing conditions were strong so that the Mn value in the oxide phase is below the detection limit. Conversely, at -215 cm (about 10.9 cal ka BP) the

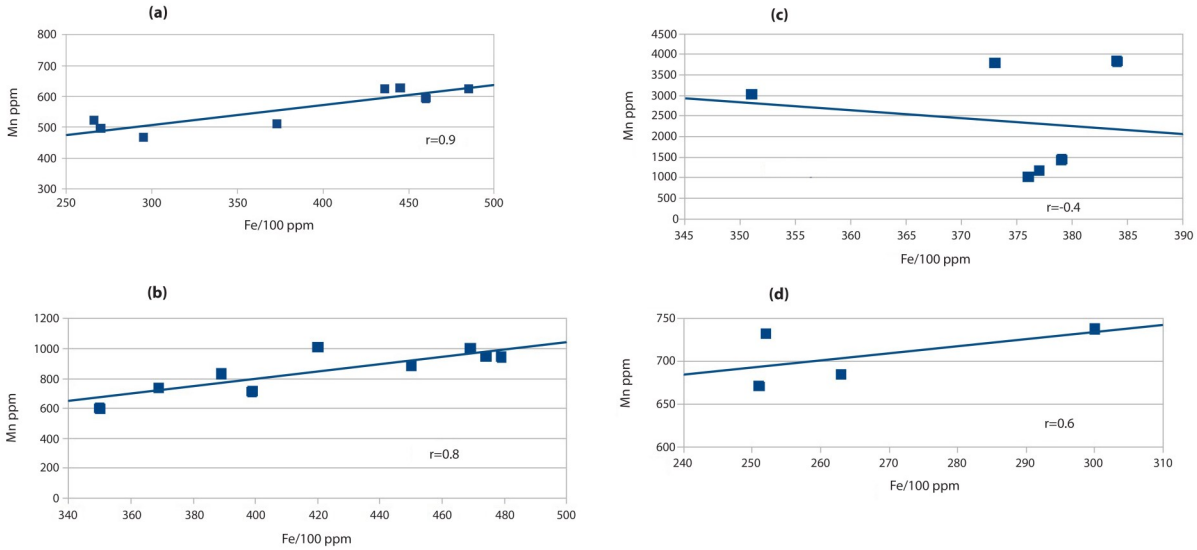

Fig. 6 - Fe-Mn correlations in Ombrone cores. a) Fe-Mn correlation in Z145 during the Glacial period. b) Fe-Mn correlation in Z145 during the Holocene period. c) Fe-Mn correlation in B60. d) Fe-Mn correlation in F12.

percentage of Mn^{+4} in the oxide fraction is higher than the percentage of the Mn^{+2} in the carbonate phase. This feature corresponds to "normal" oxidized sedimentation in a not fully marine environment, as the sea level was yet lower than the present and the sampling site was nearer to the coast.

In B60, as in Z145, most of Mn concentrates in carbonate and oxide fractions with nearly constant values of about 86-90%. In the superficial level, the Mn value in the oxide fraction reaches 41%, sharply decreasing in the sub superficial levels. Below the level -1.5 cm, Mn mainly is in the reduced form (Mn^{+2}), strongly enriched in the carbonate fraction, in agreement with fully marine condition (Glasby, 2006).

5.3. Fe

In core Z145, the Fe and Mn trends (Fig. 3b) are similar, due to the redox conditions found in this depositional environment (Williamson, 1999; Callender, 2003; Haese, 2006; Martinez-Ruiz et al., 2015). Before the Glacial-Holocene transition their values strictly correlate (r=0.9) and are still in good agreement during the first phase of the Holocene (r=0.8) (see Fig. 6 a, b). In Glacial and Holocene anoxic periods, data show very low Eh values inducing the reduction of Fe. Mn and Fe dissolve and follow the same trend. Similar correlations are found also by Olivieri et al. (2013) in anoxic sediments. After the end of the Holocene reducing layer, the onset of oxidizing conditions caused a progressive difference between the Fe and Mn trends (Fig. 3b): the Mn concentrations increase toward the top of the core, while Fe does not follow this trend. These trends also occur in recent sediments, such as in B60 and F12. In core B60, there is no correlation between Mn and Fe (Tab. 3 and Fig. 6c), because the elements have different behaviors in oxidizing conditions. Mn-Fe, instead, show a weak correlation (r=0.6) in F12 (Fig. 5d and Tab.6), due to the localization of this site near to the coast where not fully marine conditions are attained, partially hampering the precipitation of the Mn.

The mean Fe concentration in B60 (Tab. 3) is about 12% less than the Holocene mean in Z145 (Tab. 2a). A similar decrease (about 15%) is also recognizable in all other recent sediments (Tab. 4), probably due to the presence of continuous iron mining activity in the Tuscan mining district since the Etruscan age. Mineral exploitation reached the maximum during the Industrial Age and had ended by the mid-twentieth century. Mining probably caused significant decrease in the total average Fe content in the environment.

In both Z145 and B60 (Tab. 5), Fe is mainly concentrated in the residual fraction (95-99%), and it is only represented in small percentages in the organic and oxide portions. The low presence of the oxide fraction is probably due to the chemical-reducing attack that is not sufficiently strong to dissolve the iron oxides. All the Fe, then, is nearly attributed to the residual phase.

6. DISCUSSION

Chemical analyses performed in this study, together with previous isotopic and micropaleontological studies, allow the identification of two reducing layers deposited in the Central Tyrrhenian Sea. Anoxic conditions occur thanks to the favorable position of the sampling site within the continental platform, at about 150 m depth during high-stand periods, facing three river mouths, in a basin where water exchanges are weak-

Age (yr AD)	1986	1982	1967	1948
Dept (cm)	1	1,5	3,5	6
Fe/100 (ppm)	252	251	263	300
Mn (ppm)	732	671	685	738

Tab. 6 - Mn and Fe/100 concentrations in box-core F12.

ened by few submerged highs such as the Elba ridge. In this situation, the influence of the enhanced continental runoff, mostly of the Ombrone River supply, was strong enough to create reducing environments, leading to some sapropel-type levels.

6.1. Holocene Reducing Layer

Former micropaleontological and isotopic analyses (Carboni et al., 2005) and new trace element data agree in highlighting the presence of a reducing layer in the studied area during the Holocene. This anoxia period is characterized by phase of enhanced productivity (Carboni et al., 2005), with an increase of SR (Fig. 2b) from 17 to 44 cm/ka. The TOC content rises from about 0.5-0.6% up to about 1% (Ruscito personal communication), a typical value of West Mediterranean ORLs (Rogerson et al., 2008; Fink et al., 2013).

Faunal assemblages highlight a change in the marine circulation regime from well-mixed eutrophic to stratified oligotrophic waters in a temporal range spanning from about 7.4 to 5.2 cal ka BP (Carboni et al., 2005). The lighter $\delta^{18}O$ values (Tab. 1, Fig. 3) mark the increased freshwater input from 7.1 cal ka BP to slighlty after 5.7 cal ka BP. At about 6.8 cal ka BP, the reducing conditions became strong enough to produce a remarkable Pb precipitation and its concentration shows a temporal range of enrichment comprised between 6.8 and 5.7 cal ka BP, peaking at 6.2 cal ka BP (Tab. 2a, Fig. 3a). Low Mn values (Fig. 3b, Tab. 2a) suggest the presence of reducing conditions at ~6.7 cal ka BP, while the concentration peak at 6.2 cal ka BP probably does not coincide with the end of the anoxia period, but rather represents a post depositional re-oxidation of the sediment by bioturbation (Rey et al., 2008), as high Pb concentration shows that reducing conditions were present at least until 5.7 cal ka BP. This difference of about 500 years corresponds to ~ 20 cm of reworked sediment, in agreement with Reitz et al., (2006). The ranges of all proxies mostly overlap, defining the chronological boundaries of the ORL. Pb shows the narrower time span, highlighting the climax of the period between 6.8 and 5.7 cal ka BP. Among our investigated parameters, the Pb concentration, not influenced by post-depositional re-oxidation, is acknowledged to be the best marker to detect the climax of the anoxic period.

This period is almost synchronous with the Sapropel layer S1b (7.4-6.4 cal ka BP) found by Bakrač et al. (2018) in Lake Vrana (Croatia) corresponding to an increased freshwater discharge, and also with the maximum level at Lake Medina (6.2-5.8 cal ka BP) found in the SW Iberian Peninsula by Schröder et al. (2018). It also partially overlaps with a main increase of Alpine floods found by Sabatier et al. (2017), thus highlighting its regional significance over the Mediterranean Basin.

Our data agree with the enhanced rainy period recognized by many authors in the West Central Mediterranean area (Zanchetta et al., 2007; Tinner et al., 2009; Spötl et al., 2010; Zhornyak et al., 2011; Fletcher et al., 2013; Toucanne et al., 2015; Bakrac et al., 2018), taking into account some delay between the increase of precipitations on the continental sites and the development of oligotrophic and reducing conditions on the sea floor (Di Donato et al., 2019).

Holocene anoxia period found in the Ombrone submerged delta also partially overlaps with the last phases of Sapropel S1 found in the East Mediterranean (Grimm et al., 2015; Grant et al., 2016; Tesi et al., 2017; Swingedown et al., 2019; Wu et al., 2019), showing that enhanced freshwater runoff during sapropel formation was not restricted to the Eastern Mediterranean but was rather widespread over the entire Mediterranean region, including its northern borderlands. Moreover, it suggests that in the West Mediterranean region this “pluvial” period reached its maximum during the last phases of sapropel S1b formation in the East.

In the Ligurian basin (North Tyrrhenian Sea) in the 11-6 ka period, enhanced rivers activity and low ventilated bottom sea waters occurred. Moreover, during the last 6 ka, a windy cooler climate improved the bottom water reoxygenation (Le Houedec et al., 2021), in good agreement with our paleoclimatic reconstruction from the Ombrone submerged delta.

6.2. Glacial Reducing Layer

Despite the scarcer resolution due to the low sedimentation rate (Fig. 2b), at about 27.2 cal ka BP another anoxic period, of similar intensity of the Holocene one, was hypothesized basing on trace element data.

Here high Pb concentrations are found, and Pb reaches 309 ppm (Tab. 2b and Fig. 3a), a value close to that observed in the Holocene anoxic layer, about 13 times higher than the mean of other Glacial values (24 ppm). This suggests that chemical and physical conditions were similar. Based on an estimated sea level of about 120-130 m below the current one (Alessio et al., 1994; Capozzi et a., 2009; Clark et al., 2009), during the Glacial period the distance between the Ombrone River mouth and the sampling site was about 7 km and the water depth about 20-30 m. This setting emphasized the coastal supplies, although the hydrological cycle and the river runoff were probably weaker than during the Holocene.

The enhanced Pb concentration at 27.2 cal ka BP is synchronous with a phase marked by the increase of the warm-water species *G. bulloides* (Carboni et al., 2005) and by decreasing of $\delta^{18}O$ ratios (Tab. 1, Fig. 3). These data highlight a warmer and wetter fluctuation during the Late Glacial (Svensson et al., 2008; Guilizzoni et al., 2014; Oliva et al., 2018). This climatic amelioration probably induced an increased freshwater supply that produced in our area a stratified column with reducing conditions, involving Pb precipitation.

8. CONCLUSIONS

New trace element data performed on marine sediments collected on the Ombrone submerged delta (Central Tyrrhenian Sea), complement the previously published paleoenvironmental reconstruction in the area between 29 and 4.2 cal ka BP and allows the reconstruction of changing oxidation condition at the sea bottom.

Fe, Mn and Pb contents proved to be powerful tools for recognizing periods of anoxia in the basin, being particularly sensitive to environmental variations of pH and Eh conditions. We found that Pb was the most

sensitive proxy to identify environmental sapropel-type (i.e. anoxic) conditions, with total concentrations reaching high anomalous values (about 9 times the present background) during specific past periods, even though this area in the last century has been affected by anthropic pollution, mainly from mining activities and lead-added fuel that increased the natural Pb background.

In agreement with previous data, two reducing periods have been recognized. The first occurs during the Glacial at about 27,2 cal ka BP. The second occur during the Holocene between 7.4 and 5.2 cal ka BP, with a climax between 6.8 and 5.7 cal ka BP, identifying a sapropel-type sedimentation phase. The formation of the anoxic layer in the Ombrone submerged delta during the glacial period was favored by the geomorphological conditions of a semi-enclosed basin, where water exchanges with the open sea were weakened. Formation of this layer is also related to the increased vicinity of the site to the river mouth during the marine low-stand, that allowed increased freshwater supply.

The Holocene reducing layer was probably a consequence of an intense rainfall period in the West- Central Mediterranean area, representative of the climatic situation of the Northern Mediterranean region, perhaps with some influences from the Southern part of the region.

The Holocene anoxic period partially overlaps with the last phases of Sapropel S1b found in the East Mediterranean, suggesting that the humid climate during sapropel formation was not restricted to the Eastern Mediterranean, but was rather widespread over the entire Mediterranean region, although the highest rainfall phases were not strictly synchronous in the two basins.

The comparison with this paleoenvironmental reconstruction in a period not affected by human activity could help to evaluate anthropic influences in current environmental conditions and to make predictions of future developments.

ACKNOWLEDGEMENTS

We would like to thank Prof. F.L. Chiocci, who provided us with samples collected as part of the CNR marine campaigns. We also thank Prof. B. Landini and Dr C. Tarragoni for their aid in the sample classification. Dr. Voltaggio and another anonymous reviewer are acknowledged for their positive comments to the first versione of the ms.

REFERENCES

Adamson K.R., Hughes P.D., Woodward J.C. (2013) - Pleistocene glaciation of the Mediterranean Mountains. Quaternary Newsletters, 131, 1-15.

Alessio M., Allegri L., Antonioli F., Belluomini G., Improta S., Manfra L., Preite-Martinez M. (1994) - La curva di risalita del mare Tirreno negli ultimi 43 Ka ricavata da datazioni di speleotemi sommersi e dati archeologici. Memorie descrittive della Carta Geologica d'Italia, 52, 261-276.

Angelidis M.O., Radakovitch O., Veron, A., Aloupi M., Heussner S., Price B. (2011) - Anthropogenic metal contamination and sapropel imprints in deep Mediterranean sediments. Marine Pollution Bulletin, 62, 1041-1052.
Doi: 10.1016/j.marpolbul.2011.02.030

Bakrač K., Ilijanić N., Miko S., Hasan O. (2018) - Evidence of sapropel S1 formation from Holocene lacustrine sequences in Lake Vrana in Dalmatia (Croatia). Quaternary International, 494, 5-18.
Doi: 10.1016/j.quaint.2018.06.010

Bard E., Delaygue G., Rostek F., Antonioli F., Silenzi S., Schrag D.P. (2002) - Hydrological conditions over the western Mediterranean basin during the deposition of the cold Sapropel 6 (ca. 175 kyr BP). Earth and Planetary Science Letters, 202, 481-494.
Doi: 10.1016/S0012-821X(02)00788-4

Bazzicalupo P., Maiorano P., Girone A., Marino M., Combourieu-Nebout N., Incarbona A. (2018) - High-frequency climate fluctuations over the last deglaciation in the Alboran Sea, Western Mediterranean: Evidence from calcareous plankton assemblages. Palaeogeography, Palaeoclimatology, Palaeoecology, 506, 226-241.
Doi: 10.1016/j.palaeo.2018.06.042

Bellotti P., Caputo C., Davoli L., Evangelista S., Garzanti E., Pugliese F., Valeri P. (2004) - Morpho-sedimentary characteristics and Holocene evolution of the emergent part of the Ombrone River delta (southern Tuscany). Geomorphology, 61 (1-2), 71-90.
Doi: 10.1016/j.geomorph.2003.11.007

Belluomini G., Branca M., Improta S., Manfra L., Ruscito V., Vesica P., Voltaggio M. (2002) - Il sistema deltizio del Fiume Ombrone: determinazione delle velocità di sedimentazione mediante metodi radiometrici. Studi Costieri, 5, 35-45.

Bergamin L., Celia Magno M., Chiocci F.L., Di Bella L., La Monica G.B., Landini B. (2001) - Stratigrafia dell'immediato sottofondo marino antistante il fiume Ombrone. Conference Bilancio sedimentario dei sistemi costieri italiani. Processi naturali ed influenze antropiche, Porto d'Ischia, May, 15-17, 2001. Abstract Book.

Beyin A., Prendergast M.E., Grillo K.M., Wang H. (2017) - New radiocarbon dates for terminal Pleistocene and early Holocene settlements in West Turkana, northern Kenya. Quaternary Science Reviews, 30, 1-18.
Doi: 10.1016/j.quascirev.2017.04.012

Bini M., Zanchetta G., Persolu A., Cartier R., Català A., Cacho I., Dean J.R., Di Rita F., Drysdale R.N., Finnè M., Isola I., Jalali B., Lirer F., Magri D., Masi A., Marks L., Mercuri A.M., Peyron O., Sadori L., Sicre M-A., Welc F., Zielhofer C., Brisset E. (2019) - The 4.2 ka BP Event in the Mediterranean Region: an overview. Climate of the Past, 15, 555-577.
Doi: 10.5194/cp-15-555-2019

Blanchet C.L., Osborne A.H., Tjallingii R. Ehrmann W., Friedrich T., Timmermann A., Brückmann W., Frank M. (2021) - Drivers of river reactivation in North Africa during the last glacial cycle. Nature Geoscience, 14, 97-103.
Doi: 10.1038/s41561-020-00671-3

Callender E. (2003) - Heavy metals in the environment:

historical trends. In: Lollar B.S., ed. Environmental geochemistry, treatise on geochemistry. Oxford: Elsevier-Pergamon, 9, 67-105.
Doi: 10.1016/B0-08-043751-6/09161-1

Capozzi R., Negri A. (2009) - Role of sea-level forced sedimentary processes on the distribution of organic carbon-rich marine sediments: A review of the Late Quaternary sapropels in the Mediterranean Sea. Palaeogeography, Palaeoclimatology, Palaeoecology, 373, 249-257.
Doi: 10.1016/j.palaeo.2008.05.009

CappuynsV., Swennen R., Niclaes M. (2007) - Application of the BCR sequential extraction scheme to dredged pond sediments contaminated by Pb-Zn mining: A combined geochemical and mineralogical approach. Journal of Geochemical Exploration. 93, 78-90.
Doi: 10.1016/j.gex-plo.2006.10.001

Carboni M.G., Bellotti P., Bergamin L., Di Bella L., Matteucci R. (2000) - Benthic foraminiferal assemblages from the Ombrone and Tiber deltas: a preliminary comparison. Géologie Méditerranéenne, 27 (1-2), 3-13.
Doi: 10.3406/geolm.2000.1662

Carboni M.G., Bergamin L., Di Bella L., Landini B., Manfra L., Vesica P. (2005) - Late Quaternary paleoclimatic and paleoenvironmental changes in the Tyrrhenian Sea. Quaternary Science Reviews, 24, 2069-2082.
Doi: 10.1016/j.quascirev.2004.09.009

Carlson A.E. (2013) - The Younger Dryas Climate Event in “The Encyclopedia of Quaternary Science”, 3, 126-134. Elias S.A. (Ed), Elsevier.
Doi: 10.1016/B978-0-444-53643-3.00029-7

Clark P.U., Dyke A.S., Shakun J.D., Carlson A.E., Clark J., Wohlfarth B., Mitrovica J.X., Hostetler S.W., McCabe A.M. (2009) - The Last Glacial Maximum. Science, 325, 710-714.

Colonese A.C., Zanchetta G., Fallik A.E., Manganelli G., Saña M., Alcade G., Nebot J. (2013) - Holocene snail shell isotopic record of millennial-scale hydrological conditions in western Mediterranean: Data from Bauma del Serrat del Pont (NE Iberian Peninsula). Quaternary International, 303, 43-53.
Doi: 10.1016/j.quaint.2013.01.019

Conforto L., Manfra L. (2004) - Heavy metals chronological and area trends of shelf marine sediments in Central Tyrrhenian Sea (Tuscany Italy). Geochimica et Cosmochimica Acta. Abstract of the 13th Goldschmit Conference, A524.4.65. P03.

Conforto L, Manfra L. (2007) - Heavy metals in the submerged Ombrone river delta (Central Tyrrhenian Sea - Italy). Geoitalia. Sesto Forum Italiano di Scienze della Terra, 71.

Conforto L., Manfra L., Corrado L. (2008) - Holocene and present-days heavy metals in Central Tyrrhenian Sea sediments. 33° International Geological Congress Oslo. Poster.

Di Donato V., Insinga D.D., Iorio M., Molisso F., Rumolo P., Cardines C., Passaro S. (2019) - The palaeoclimatic and palaeoceanographic history of the Gulf of Taranto (Mediterranean Sea) in the last 15 ky. Global Planetary Change, 172, 278-297.
Doi: 10.1016/j.gloplacha.2018.10.014

Di Rita F., Fletcher W.J., Aranbarri J., Margaritelli G., Lirer F., Magri D. (2018) - Holocene forest dynamics in central and western Mediterranean: periodicity, spatio-temporal patterns and climate influence. Scientific Reports, 8, 8929.
Doi: 10.1038/s41598-018-27056-2

Domínguez-Villar D., Carrasco R.M., Pedraza J., Cheng H., Edwards R.L., Willenbring J.K. (2013) - Early maximum extent of paleoglaciers from Mediterranean mountains during the last glaciation. Scientific Reports, 3, 2034.
Doi: 10.1038/srep02034

Drab L., Carlut J., Hubert-Ferrari A., Martinez P., Le-Point G., El Ouahabi M. (2015) - Paleomagnetic and geochemical record from cores from the Sea of Marmara, Turkey: Age constraints and implications of sapropelic deposition on early diagenesis. Marine Geology, 360,40-54.
Doi: 10.1016/j.margeo.2014.12.002

Dubois-Dauphin Q., Montagna P., Siani G., Douville E., Wienberg C., Hebbeln D., Liu Z., Kallel N., Dapoigny A., Revel M., Pons-Branchu E., Taviani M., Colin C. (2017) - Hydrological variations of the intermediate water masses of the western Mediterranean Sea during the past 20 ka inferred from neodymium isotopic composition in foraminifera and cold-water corals. Climate of the Past, 13, 17-37.
Doi: 10.5194/cp-13-17-2017

Fiedel S.J. (2011). The mysterious onset of the Younger Dryas. Quaternary International, 242, 262-266.
Doi: 10.1016/j.quaint.2011.02.044

Filippidi A., Triantaphyllou M.V., De Lange G.J. (2016) - Eastern-Mediterranean variability during sapropel S1 formation, evaluated at two sites influenced by deep-water formation from Adriatic and Aegean Seas. Quaternary Science Reviews, 144, 95-106.
Doi: 10.1016/j.quascirev.2016.05.024

Fink H.G., Wienberg C., De Pol-Holz R., Wintersteller P., Hebbeln D. (2013) - Cold-water coral growth in the Alboran Sea related to high productivity during the Late Pleistocene and Holocene. Marine Geology, 339, 71-81.
Doi: 10.1016/j.margeo.2013.04.009

Fletcher W.K. (1981) - Analytical Methods in Geochemical Prospecting. Handbook of Exploration Geochemistry,1. Elsevier, Amsterdam, Holland.

Gallego-Torres D., Martinez-Ruiz F., de Lange G.J., Jimenéz-Espejo F.J., Ortega-Huertas M. (2010) - Trace-elemental derived paleoceanographic and paleoclimatic conditions for Pleistocene Eastern Mediterranean sapropels. Palaeogeography, Palaeoclimatology, Palaeoecology, 293, 76-89.
Doi: 10.1016/j.palaeo.2010.05.001

Geraga M., Ioakim C. Lykousis V., Tsaila-Monopolis S., Mylona G. (2010) - The high-resolution palaeoclimatic and palaeocenographic history of the last 24,000 years in the central Aegean Sea, Greece. Palaeogeography, Palaeoclimatology, Palaeoecology, 287, 101-115.
Doi: 10.1016/j.palaeo.2010.01.023

Glasby G.P. (2006) - Manganese: Predominant Role of

Nodules and Crust. Marine Geochemistry. Schulz H.D., Zabel M. (Eds), Springer- Berlin-Heidelberg-New York, 371-415.
Doi: 10.1007/3-540-32144-6_11

Grant K.M., Grimm R., Mikolajewicz U., Marino G., Ziegler M., Rohling E.J. (2016) - The timing of Mediterranean sapropel deposition relative to insolation, sea-level and African monsoon changes. Quaternary Science Reviews, 140, 125-141.
Doi: 10.1016/j.quascirev.2016.03.026

Grimm R., Maier-Reimer E., Mikolajewicz U., Schmiedl G., Müller-Navarra K., Adloff F. M., Grant K.M., Ziegler M., Lourens L.J., Emeis K.C. (2015) - Late glacial initiation of Holocene eastern Mediterranean sapropel formation. Nature Communications, 6, Article number: 7099.
Doi: 10.1038/ncomms8099

Gromig R., Mechernich S., Ribolini A., Wagner B., Zanchetta G., Isola I., Bini M., Dunai T.J. (2018) - Evidence for a Younger Dryas deglaciation in the Galicia Mountains (FYROM) from cosmogenic 36Cl. Quaternary International, 464, 352-363.
Doi: 10.1016/j.quaint.2017.07.013

Guilizzoni P., Lami A., Marchetto A., Ariztegui D. (2014) - Lakes. In: Litho-paleaoenvironmental maps of Italy during the last two climate extremes. Researchgate.net/publication/262484813.

Haese R.R. (2006) - The Reactivity of the Iron. Marine Geochemistry, Schulz H.D., Zabel M., (Eds), Springer- Berlin-Heidelberg- New York, 241-264.

Heimbürger L.E., Cossa D., Thibodeau B., Khripounoff A., Mas, V., Chiffoleau J.F., Schmidt S., Migon C. (2012) - Natural and anthropogenic trace metals in sediments of the Ligurian Sea (Northwestern Mediterranean). Chemical Geology, 291, 141-151.
Doi: 10.1016/j.chemgeo.2011.10.011

Hennekam R., Jilbert T., Schnetger B., de Lange G.J. (2014) - Solar forcing of Nile and sapropel S1 formation in the early to middle Holocene eastern Mediterranaean. Paleoceanography and Paleoclimatology, 29 (5), 343-356.

Incarbona A., Sprovieri M. (2020) - The postglacial isotopic record of intermediate water connects Mediterranean Sapropels and organic-rich layers. Paleoceanography and Paleoclimatology, 35, 1-20.
Doi: 10.1029/2020PA004009

Isola I., Zanchetta G., Drysdale R.N., Regattieri E., Bini M., Bajo P., Hellstrom J.C., Baneschi I., Lionello P., Woodhead J., Greig A. (2019) - The 4.2 ka BP event in the Central Mediterranean: New data from Corchia speleothems (Apuan Alps, central Italy). Climate of the Past, 15, 135-154.
Doi: 10.5194/cp-15-135-2019

Ivy-Ochs S., Kerschner H., Reuther A., Preusser F., Heine K., Maisch M., Kubik P.W., Schlüchter C., (2008) - Chronology of the last glacial cycle in the European Alps. Journal of Quaternary Science, 23 (6-7), 559-573.
Doi: 10.1002/jqs.1202

Jiménez-Espejo F.J., Pardos-Gené M., Martínez-Ruiz F., García-Alix A., van de Flierdt T., Toyofuku T., Bahr A., Kreissig K. (2015) - Geochemical evidence for intermediate water circulation in the westernmost Mediterranean over the last 20 kyr BP and its impact on the Mediterranean Outflow. Global Planetary Change, 135, 38-46.
Doi: 10.1016/j.gloplacha.2015.10.001

Kandiano E.S., Bauch H.A., Fahl K. (2014) - Last interglacial surface water structure in the western Mediterranean (Balearic) Sea: Climatic variability and link between low and high latitudes. Global and Planetary Change, 123(A), 67-76.
Doi: 10.1016/j.gloplacha.2014.10.004

Keigwin L.D., Klotsko S., Zhao N., Reilly B., Giosan L., Driscoll N.W. (2018) - Deglacial floods in the Beaufort Sea preceded Younger Dryas cooling. Nature Geoscience, 11, 599-604.
Doi: 10.1038/s41561-018-0169-6

Kennet D.J., Aura Tortosa J.E., Bischoff J.L. Daniel I.R., Erlandson S. (2015) - Bayesian chronological analyses consistent with synchronous age of 12,835-12,735 Cal B.P. for Younger Dryas Boundary on four continents. Proceedings of the National Academy of Sciences (PNAS), 112, 4344-4353.
Doi: 10.1073/pnas.150714611

Kidd R.B., Cita M.B., Ryan W.B.F. (1978) - Stratigraphy of eastern Mediterranean sapropel sequences recovered during DSDP Leg 142 and their paleoenvironmental significance. Initial Reports of the Deep Sea Drilling Project, 42, 421-443.

Kotthoff U., Pross J., Müller U.C., Peyron O., Schmiedl G., Schulz H., Bordon A. (2008) - Climate dynamics in the borderlands of the Aegean Sea during formation of sapropel S1 deduced from a marine pollen record. Quaternary Science Reviews, 27, 832-845.
Doi: 10.1016/j.quascirev.2007.12.001

Le Houedec S., Mojtahid M., Ciobanu M., Jorry S.J., Bouhdayad F.Z., Guyonneau E., Sourice S., Toucanne S. (2021) - Deglacial to Holocene environmental changes in the northern Ligurian Sea: The dual influence of regional climate variability and large-scale intermediate Mediterranean circulation. Palaeogeography, Palaeoclimatology, Palaeoecology, 576, 110500.
Doi: g/10.1016/j.palaeo.2021.110500

Lionello P., Malanotte-Rizzoli P., Boscolo R. (Eds.) (2006) - Mediterranean climate variability. Elsevier.

Lirer F., Sprovieri M., Ferraro L., Vallefuoco M., Capotondi L., Cascella A., Petrosino P., Insinga D.D., Pelosi N., Tamburrino S., Lubritto C. (2013) - Integrated stratigraphy for the Late Quaternary in eastern Tyrrhenian Sea. Quaternary International, 292, 71-85.
Doi: 10.1016/j.quaint.2012.08.2055

Magny M., Vannière B., Calo C., Millet L., Leroux A., Peyron O., Zanchetta G., La Mantia T., Tinner W. (2011) - Holocene hydrological changes in southwestern Mediterranean as recorded by lake-level fluctuations at Lago Preola, a coastal lake in southern Sicily, Italy. Quaternary Science Reviews, 30, 2459-2473.
Doi: 10.1016/j.quascirev.2011.05.018

Martinez-Ruiz F., Kastner M., Gallego-Torres M., Ortega-Huertas M. (2015) - Paleoclimate and paleoceanography over the past 20,000 yr in the Mediterra-

nean Sea Basin as indicated by sediment elemental proxies. Quaternary Science Reviews, 107, 25-46.
Doi: 10.1016/j.quascirev.2014.09.018

McCulloch M., Taviani M., Montagna P., López Correa M., Remia A., Mortimer G. (2010) - Proliferation and demise of deep-sea corals in the Mediterranean during the Younger Dryas. Earth and Planetary Science Letters, 298, 143-152.
Doi: 10.1016/j.epsl.2010.07.036

Melki T., Kallel N., Jorissen F.J., Guichard F., Dennielou B., Berné S., Labeyrie L., Fontugne M. (2009) - Abrupt climate change, sea surface and paleoproductivity in the western Mediterranean Sea (gulf of Lion) during the last 28 Kyr. Palaeogeography, Palaeoclimatology, Palaeoecology, 279, 96-113.
Doi: 10.1016/j.palaeo.2009.05.005

Mihaljevic M. (1999) - Lead. Encyclopedia of Geochemistry. Marshall C.P., Fairbridge R.W. (Eds), Kluwer Academic Publishers Dordrecht-Boston, 362-363.

Naimo D., Adamo P., Imperato M., Stanzione D. (2005) - Mineralogy and geochemistry of a marine sequence, Gulf of Salerno Italy. Quaternary International, 140, 53-63.
Doi: 10.1016/j.quaint.2005.05.004

Negri A., Colleoni F., Masina S. (2012) - Mediterranean sapropels: a mere geological problem or a resource for the study of a changing planet ? Alpine and Mediterranean Quaternary, 25 (2), 81-89.

Oliva M., Žebre M., Guglielmin M., Hughes P.D., Çiner A., Vieira G., Bodin X., Andrés N., Colucci R.R., García-Hernández C., Mora C., Nofre J., Palacio D., Pérez-Alberti A., Ribolini A., Ruiz-Fernández J., Sarıkaya M.A, Serrano E., Urdea P., Valcárcel M., Woodward J.C., Yıldırım C. (2018) - Permafrost conditions in the Mediterranean region since the Last Glaciation. Earth-Science Reviews, 185, 397-436.
Doi: 10.1016/j.earscirev.2018.06.018

Olivieri E., Sprovieri M., Manta D.S., Giaramita L., La Cono V., Lirer F., Rumolo P., Sabatino N., Tranchida G., Vallefuoco M., Yakimov M.M., Mazzola S. (2013) - Sediment geochemistry of the Thetis hypersaline anoxic basin (eastern Mediterranean Sea). Sedimentary Geology, 296, 72-85.
Doi: 10.1016/j.sedgeo.2013.08.007

Pasquier V., Toucanne S., Sansjofre P., Dixit Y., Revillon S., Mokeddem Z., Rabineau M. (2019) - Organic matter isotopes reveal enhanced rainfall activity in Northwestern Mediterranean borderland during warm substages of the last 200 kyr. Quaternary Science Reviews, 205, 182-192.
Doi: 10.1016/j.quascirev.2018.12.007

Pauly M., Helle G., Miramont C., Büntgen U., Treydt K., Reinig F., Guibal F., Sivan O., Heinrich I., Riedel F., Kromer B., Balanzategu D., Wacker L., Sookdeo A., Brauer A. (2018) - Subfossil trees suggest enhanced Mediterranean hydroclimate variability at the onset of the Younger Dryas. Scientific Report, 8, 13980.
Doi: 10.1038/s41598-018-32251-2

Pérez Asensio J.N., Frigola J., Pena L.D., Sierra F.J., Reguera M.I., Rodrfguez-Tovar F.J., Dorador J., Asioli A., Kuhlmann J., Huhn K., Cacho I. (2020) - Changes in western Mediterranean thermohaline circulation in association with a deglacial Organic Rich Layer formation in the Alboran Sea. Quaternary Science Reviews, 228, 103527.
Doi: 10.1016/j.quascirev.2019.106075

Petrie L.M. (1999) - Manganese. Encyclopedia of Geochemistry. Marshall C.P., Fairbridge R.W. (Eds), Kluwer Academic Publishers Dordrecht-Boston, 382-384.

Reimer P.J., Austin W.E.N., Bard E., Bayliss A., Blackwell P.G., Bronk Ramsey C.B., Butzin M., Cheng H., Edwards R.L., Friedrich M., Grootes P.M., Guilderson T.P., Hajdas I., Heaton T.J., Hogg A.G., Hughen K.A., Kromer B., Manning S.W., Muscheler R., Palmer J.G., Pearson C., van der Plicht J., Reimer R.W., Richards D.A., Scott E.M., Southon J.R., Turney C.S.M., Wacker L., Adolphi F., Büntgen U., Capano M., Fahrni S.M., Fogtmann-Schulz A., Friedrich R., Köhler P., Kudsk S., Miyake F., Olsen J., Reinig F., Sakamoto M., Sookdeo A., Talamo, S. (2020) - The IntCal20 Northern Hemisphere Radiocarbon Age Calibration Curve (0-55 cal kBP). Radiocarbon, 62(4), 725-757.
Doi: 10.1017/RDC.2020.41

Reitz A., Thomson J., De Lange G., Hensen C. (2006) - Source and development of large manganese enrichments above eastern Mediterranean sapropel S1. Paleocenography and Paleoclimatology, 21, PA 3007.
Doi: 10.1029/2005PA001169

Rey D., Rubio B., Mohamed K., Vilas F., Alonso B., Ercilla G., Rivas T. (2008) - Detrital and early diagenetic processes in the Late Pleistocene and Holocene sediments from the SW Galicia Bank inferred from high-resolution enviromagnetic and geochemical records. Marine Geology, 249, 64-92.
Doi: 10.1016/j.margeo.2007.09.013

Ribolini A., Bini M., Isola I., Spagnolo M., Zanchetta G., Pellitero R., Mechernich S., Gromig R., Dunai T., Wagner B., Milevski I. (2018) - An Oldest Dryas glacier expansion on Mount Pelister (Former Yugoslavian Republic of Macedonia) according to 10Be cosmogenic dating. Journal of the Geological Society, 175, 100-110.
Doi: 10.1144/jgs2017-038

Rodrigo-Gámiz M., Martinez-Ruiz F., Jimenés-Espejo F.J., Gallego-Torres D., Nieto-Moreno V., Romero O., Ariztegui D. (2011) - Impact of climate variability in the western Mediterranean during the last 20,000 years: oceanic and atmospheric responses. Quaternary Science Reviews, 30, 2018-2034.
Doi: 10.1016/j.quascirev.2011.05.011

Rogerson M., Cacho I., Jimenéz-Espejo F., Reguera M. I., Sierro F.J., Martinez-Ruiz F., Frigola J., Canals M. (2008) - A dynamic explanation for the origin of the western Mediterranean organic-rich layers. Geochemistry Geophysics Geosystems, 9(7), Q07U01.
Doi: 10.1029/2007GC001936

Rohling E.J. (1994) - Review and new aspects concern-

ing the formation of eastern Mediterranean sapropels. Marine Geology, 122, 1-28.
Doi: 10.1016/0025-3227(94)90202-X

Rohling E.J., Hilgen F.J. (1991) - The eastern Mediterraneanclimate at times of sapropel formation: a review. Netherlands Journal of Geosciences, 70, 253 -26

Rohling E.J., Pälike H. (2005) - Centennial-scale climate cooling with a sudden cold event around 8,200 years ago. Nature, 434, 975-979.
Doi: 10.1038/nature03421

Rohling E.J., Marino G., Grant K.M. (2015) - Mediterranean climate and oceanography, and the periodic development of anoxic events (sapropel). Earth-Science Reviews, 143, 62-97.
Doi: 10.1016/j.earscirev.2015.01.008

Rossignol-Strick M. (1985) - Mediterranean Quaternary sapropels, an immediate response of the African monsoon to variation of insolation. Palaeogeography, Palaeoclimatology, Palaeoecology, 49, Issues 3-4, 237-263.
Doi: 10.1016/0031-0182(85)90056-2

Rossignol-Strick M., Nesteroff W., Olive P., Vergnaud-Grazzini C. (1982) - After the deluge: Mediterranean stagnation and sapropel formation. Nature, 295, 105-110.
Doi: 10.1038/295105a0

Roveri M., Correggiari A. (2004) - Submerged depositional terraces in the Tuscan Archipelago (Eastern margin of the Corsica Basin). Memorie Descrittive della Carta Geologica d'Italia, 58, 11-16.

Sabatier P., Wilhelm B., Ficetola G.F., Moiroux F., Poulenard J., Develle A.-L., Bichet A., Chen W., Pignol C., Reyss J-L., Gielly L., Bajard M., Perrette Y., Malet E., Taberlet P., Arnaud F. (2017) - 6-kyr record of flood frequency and intensity in the western Mediterranean Alps - Interplay of solar and temperature forcing. Quaternary Science Reviews, 170, 121-135.
Doi: 10.1016/j.quascirev.2017.06.019

Sahuquillo A.J.F., López-Sánchez R., Rubio G., Rauret R.P., Thomas C.M., Davidson A., Ure M. (1999) - Use of a certified reference material for extractable trace metals to assess sources of uncertainty in the BCR three-stage sequential extraction procedure. Analytica Chimica Acta, 382, 317-327.
Doi: 10.1016/S0003-2670(98)00754-5

Sarikaya M.S., Çiner A. (2015) - Late Quaternary glaciations in the eastern Mediterranean. Geological Society, London, Special Publications, 433, 289-305.
Doi: 10.1144/SP433.4

Schemmel F., Niedermeyer E.M., Schwab V.F., Gleixner G., Pross J., Mulch A. (2016) - Plant wax δD values record changing Eastern Mediterranean atmospheric circulation patterns during the 8.2 kyr B.P. climatic event. Quaternary Science Reviews, 133, 96-107.
Doi: 10.1016/j.quascirev.2015.12.019

Schröder T., van't Hoff J., Lopez-Saez J.A., Viehberg F., Melles M., Reicherter K. (2018) - Holocene climatic and environmental evolution on the southwestern Iberian Peninsula: A high-resolution multi-proxy study from Lake Medina (Cadiz, SW Spain). Quaternary Science Reviews, 198, 208-225.
Doi: 10.1016/j.quascirev.2018.08.030

Seguinot J., Ivy-Ochs S., Jouvet G., Huss M., Funk M., Preusser F. (2018) - Modelling last glacial cycle ice dynamics in the Alps. The Cryosphere, 12, 3265-3285.
Doi: 10.5194/tc-12-3265-2018

Shakun J.D., Carlson A.E. (2010) - A global perspective on Last Glacial Maximum to Holocene climate change. Quaternary Science Reviews, 29, 1801-1816.
Doi: 10.1016/j.quascirev.2010.03.016

Spötl C., Nicolussi K., Patzelt G., Boch R., Team D. (2010) - Humid climate during deposition of sapropel S1 in the Mediterranean Sea: Assessing the influence on the Alps. Global and Planetary Change, 71, 242-248.
Doi: 10.1016/j.gloplacha.2009.10.003

Svensson A., Andersen K.K., Bigler M., Clausen H.B., Dahl-Jensen D., Davies S.M., Johnsen S.J., Muscheler R., Parrenin F., Rasmussen S.O., Röthlisberger R., Seierstad I., Steffensen J.P., Vinther M.B. (2008) - A 60000 year Greenland stratigraphic ice core chronology. Climate of the Past, 4, 47-57.
Doi: 10.5194/cp-4-47-2008

Tesi T., Asioli A., Minisini D., Maselli V., Dalla Valle G., Gamberi F., Langone L., Cattaneo A., Montagna P., Trincardi F. (2017) - Large-scale response of the Eastern Mediterranean thermohaline circulation to African monsoon intensification during sapropel S1 formation. Quaternary Science Reviews, 159, 139-154.
Doi: 10.1016/j.quascirev.2017.01.020

Thomson J., Higgs N.C., Wilson T.R.S., Croudace I.W., de Lange G.J., van Santvoort P.J.M. (1995) - Redistribution and geochemical behaviour of redox-sensitive elements around S1, the most recent eastern Mediterranean sapropel. Geochimica et Cosmochimica Acta, 59, 3487-3501.
Doi: 10.1016/0016-7037(95)00232-O

Tinner W., van Leeuwen J.F.N., Colombaroli D., Vescovi E., van der Knaap W.O., Henne P.D., Pasta S., D'Angelo S., La Mantia T. (2009) - Holocene environmental and climatic changes at Gorgo Basso, a coastal lake in southern Sicily, Italy. Quaternary Science Reviews, 28, 1498-1510.
Doi: 10.1016/j.quascirev.2009.02.001

Tortora P. (1999) - Sediment distribution on the Ombrone River Delta seafloor anrelated dispersal processes. Geologica Romana, 35, 211-218.

Toucanne S., Angue Minto'o C.M., Fontanier C., Bassetti M. A., Jorry S.J., Jouet G. (2015) - Tracking rainfall in the northern Mediterranean borderlands during sapropel deposition. Quaternary Science Reviews, 129, 178-195.
Doi: 10.1016/j.quascirev.2015.10.016

Triantaphyllou M.V. (2014) - Coccolithophore assemblages during the Holocene Climatic Optimum in the NE Mediterranean (Aegean and northern Levantine Seas, Greece): Paleoceanographic and paleoclimatic implications. Quaternary Internation-

al, 345, 1-12.
Doi: 10.1016/j.quaint.2014.01.033

Tribovillard N., Algeo T.J., Lyons T., Riboulleau A. (2006) - Trace metals as paleoredox and paleoproductivity proxies: An update. Chemical Geology, 232, 12-13.
Doi: 10.1016/j.chemgeo.2006.02.012

Trigo I.F., Bigg G.R., Trevor D.D. (2002) - Climatology of Cyclogenesis Mechanisms in the Mediterranean. Monthly Weather Review, 130, 3, 549-569.
Doi: 10.1175/1520-0493(2002)130<0549:COCMIT>2.0.CO;2

Turner P., Margaritz M. (1986) - Chemical and isotopic studies of a core of Marl Slate from NE England: influence of freshwater influx into the Zechstein Sea. Geological Society, London, Special Publications, 22, 1, 19-29.
Doi: 10.1144/GSL.SP.1986.022.01.03

Wagner B., Vogel H., Francke A., Friedrich T., Donders T., Lacey J.H., Leng M.J., Regattieri E., Sadori L., Wilke T., Zanchetta G., Albrecht C., Bertini A., Combourieu-Nebout N., Cvetkoska A., Giaccio B., Grazhdani A., Hauffe T., Holtvoeth J., Joannin S., Jovanovska E., Just J., Kouli K., Kousis I., Koutsodendris A., Krastel S., Lagos M., Leicher N., Levkov Z., Lindhorst K., Masi A., Melles M., Mercuri A.M., Nomade S., Nowaczyk N., Panagiotopoulos K., Peyron 0., Reed J.M., Sagnotti L., Sinopoli G., Stelbrink B., Sulpizio R., Timmermann A., Tofilovska S., Torri P., Wagner-Cremer F., Wonik T., Zhan X. (2019) - Mediterranean winter rainfall in phase with African monsoons during the past 1.36 million years. Nature, 573, 256-260.
Doi: 10.1038/s41586-019-1529-0

Warning B., Brumsack H.J. (2000) - Trace metals signatures of eastern Mediterranean sapropels. Palaeogeography, Palaeoclimatology, Palaeoecology, 158, 293- 309.
Doi: 10.1016/S0031-0182(00)00055-9

Williamson M.A. (1999) - Iron. Encyclopedia of Geochemistry. Marshall C.P., Fairbridge R.W. (Eds), Kluwer Academic Publishers Dordrecht-Boston, 348-353.

Williams M.A.J., Duller G.A.T., Williams F.M., Woodward J.C., Macklin M.G., El Tom O.A.D., Munro R.N., El Hajaz Y., Barrows T.T. (2015) - Causal links between Nile floods and eastern Mediterranean sapropel formation during the past 125 kyr confirmed by OLS and radiocarbon dating of Blue and White Nile sediments. Quaternary Science Reviews, 130, 89-108.
Doi: 10.1016/j.quascirev.2015.05.024

Wu J., Liu Z., Stuut J.B.W., Zhao Y., de Lange G.J. (2017) - North-African paleodrainage discharges to central Mediterranean during the last 18,000 years: A multiproxy characterization. Quaternary Science Reviews, 163, 95-113.
Doi: 10.1016/j.quascirev.2017.03.015

Wu J., Pahnkec K., Böningc P., Wu L., Michardd A., de Lange G.J. (2019) - Divergent Mediterranean seawater circulation during Holocene sapropel formation - Reconstructed using Nd isotopes in fish debris and foraminifera. Earth and Planetary Science Letters, 511, 141-153.
Doi: 10.1016/j.epsl.2019.01.036

Zanchetta G., Drysdale R.N., Hellstrom J.C., Fallick A.E., Isola I., Gagan M.K., Pareschi M.T. (2007) - Enhanced rainfall in the Western Mediterranean during deposition of sapropel S1: stalagmite evidence from Corchia cave (Central Italy). Quaternary Science Reviews, 26, 279-286.
Doi: 10.1016/j.quascirev.2006.12.003

Zhang C., Yu Z.-g, Zeng G.-m., Jiang M., Yang Z.-z., Cui F., Zhu M.-y., Shen L.-q., Hu L. (2014) - Effect of sediment geochemical properties on heavy metal bioavailability . Environmental International, 73, 270-280.
Doi: 10.1016/j.evint.2014.08.010

Zhornyak L.V., Zanchetta G., Drysdale R.N., Hellstrom J.C., Isola I., Regattieri E., Piccini L., Baneschi I., Couchoud I. (2011) - Stratigraphic evidence for a “pluvial phase” between ca 8200-7100 ka from Renella cave (Central Italy). Quaternary Science Reviews, 30, 409-417.
Doi: 10.1016/j.quascirev.2010.12.003

Ms. received: April 17, 2024 *Revised: May 17, 2024*
Accepted: May 24, 2024 *Available online: June 14, 2024*